The Astrophysical Journal Letters, 869:L35 (6pp), 2018 December 20 https://doi.org/10.3847/2041-8213/aaf053

Viscous-dynamical Ejecta from Binary Neutron Star Mergers

David Radice[1,2], Albino Perego[3,4], Kenta Hotokezaka[2], Sebastiano Bernuzzi[3,5], Steven A. Fromm[6], and Luke F. Roberts[6]
[1] Institute for Advanced Study, 1 Einstein Drive, Princeton, NJ 08540, USA
[2] Department of Astrophysical Sciences, Princeton University, 4 Ivy Lane, Princeton, NJ 08544, USA
[3] Istituto Nazionale di Fisica Nucleare, Sezione Milano Bicocca, gruppo collegato di Parma, I-43124 Parma, Italy
[4] Dipartimento di Fisica, Università degli Studi di Milano Bicocca, Piazza della Scienza 3, I-20126 Milano, Italia
[5] Theoretisch-Physikalisches Institut,Friedrich-Schiller-Universität Jena, D-07743, Jena, Germany
[6] NSCL/FRIB and Department of Physics & Astronomy, Michigan State University, 640 South Shaw Lane East Lansing, MI 48824, USA
Received 2018 October 7; revised 2018 October 30; accepted 2018 November 7; published 2018 December 19

Abstract

General-relativistic simulations of binary neutron star (NS) mergers with viscosity reveal a new outflow mechanism operating in unequal mass binaries on dynamical timescales and enabled by turbulent viscosity. These "viscous-dynamical" ejecta are launched during the merger due to the thermalization of mass exchange streams between the secondary and the primary NS. They are characterized by asymptotic velocities extending up to $\sim 0.8c$, and have masses that depend on the efficiency of the viscous mechanism. Depending on the unknown strength of the effective viscosity arising from magnetohydrodynamic instabilities operating during the merger, the overall mass of the dynamical ejecta could be enhanced by a factor of a few and the mass of the fast tail of the ejecta, having asymptotic velocities $\geqslant 0.6c$, by up to four orders of magnitude. The radioactive decay of the expanding viscous-dynamical ejecta could produce bright kilonova transients with signatures of free neutron decay in the first hour, and enhanced near-infrared flux on a timescale of a few days. The synchrotron remnant produced by the interaction between the ejecta and the interstellar medium could also be significantly enhanced by viscosity. Such a remnant could be detected in the case of GW170817 as a rebrightening of the radio signal in the next months to years.

Key words: hydrodynamics – stars: neutron

1. Introduction

The ultraviolet (UV)/optical/infrared (IR) counterpart (Chornock et al. 2017; Cowperthwaite et al. 2017; Drout et al. 2017; Nicholl et al. 2017; Perego et al. 2017; Tanaka et al. 2017; Tanvir et al. 2017; Villar et al. 2017; Waxman et al. 2017) of the binary neutron star (NS) merger event GW170817 (Abbott et al. 2017a, 2017b, 2018b) is thought to have been powered by the radioactive decay of about $0.05\,M_\odot$ of material ejected during and shortly after the merger (Lattimer & Schramm 1974; Symbalisty & Schramm 1982; Eichler et al. 1989; Meyer 1989; Freiburghaus et al. 1999; Goriely et al. 2011; Korobkin et al. 2012; Wanajo et al. 2014; Just et al. 2015; Kasen et al. 2017; Thielemann et al. 2017; Hotokezaka et al. 2018a; Rosswog et al. 2018), the so-called kilonova (KN).

The observations can be fitted with a minimal two-components KN model (Chornock et al. 2017; Cowperthwaite et al. 2017; Drout et al. 2017; Nicholl et al. 2017; Tanaka et al. 2017; Tanvir et al. 2017; Villar et al. 2017; see, however, Waxman et al. 2017 for an alternative model). The first component, often called the "blue KN," peaked on a short timescale ($\sim$1 day from the merger) in the UV/optical bands and is thought to have been powered by the radioactive decay of $\sim 0.02\,M_\odot$ of low photon-opacity material with a large expansion velocity $\sim 0.3c$. The second component, typically referred to as the "red KN," peaked on a timescale of $\sim$5 days in the near-IR (NIR) bands and is thought to have been powered by the radioactive decay of $\sim 0.04\,M_\odot$ of high-photon-opacity material characterized by a lower expansion velocity $\sim 0.1c$. This minimal model is, however, incompatible with general-relativistic hydrodynamic (GRHD) merger simulations that cannot produce a sufficient amount of fast-moving ejecta (e.g., Davies et al. 1994; Bauswein et al. 2013; Hotokezaka et al. 2013; Rosswog et al. 2013; Radice et al. 2016). This discrepancy could point to the presence of additional physics beyond that included in the simulations, such as the presence of magnetized winds from the merger remnant (Fernández et al. 2018; Metzger et al. 2018). KN models including anisotropy, multiple ejecta components, and their interactions can only partially reconcile observations and simulations (e.g., Perego et al. 2017; Kawaguchi et al. 2018).

Merger simulations showed that binary NS mergers generate outflows through a number of different mechanisms operating on different timescales. The dynamical ejecta are launched during the merger by tidal interactions and shocks exerted on the NSs on a dynamical timescale (e.g., (Rosswog et al. 1999; Rosswog & Davies 2003; Bauswein et al. 2013; Hotokezaka et al. 2013; Wanajo et al. 2014; Sekiguchi et al. 2015, 2016; Radice et al. 2016). They have masses of $\sim 10^{-4}$–$10^{-2}\,M_\odot$ and typical velocities distributed in $\sim$0.1–0.3c with $\sim 10^{-6}$–$10^{-5}\,M_\odot$ of fast ejecta having velocities larger than $0.6c$. The superposition of dynamical ejecta launched by different mechanisms results in an outflow with a wide range of electron fractions $0.05 < Y_e < 0.4$, with higher Y_e material being typically channeled in the polar directions (see the detailed discussion in Radice et al. 2016, 2018b).

Neutrino re-absorption by material ablated from the surface of the hypermassive neutron star (HMNS) and/or from the accretion disk originates another outflow component channeled along the polar direction $\theta \lesssim 45°$ with $Y_e > 0.25$ (Dessart et al. 2009; Perego et al. 2014, 2017a, 2017b; Just et al. 2015; Martin et al. 2015). More material is also expected to be unbound by viscous and nuclear processes in the remnant's accretion disk (Metzger et al. 2008, 2009, 2018; Lee et al. 2009; Fernández & Metzger 2013; Metzger & Fernández 2014; Siegel et al. 2014; Martin et al. 2015; Wu et al. 2016; Fujibayashi et al.

2017, 2018; Lippuner et al. 2017; Siegel & Metzger 2017; Fernández et al. 2018; Siegel & Metzger 2018; Radice et al. 2018a). These additional secular ejecta are expected to provide a dominant contribution to the KN on timescales of days to weeks, while the dynamical ejecta discussed above mostly contributes to the early $\sim$1 day emission (Radice et al. 2018b). The presence of a fast dynamical ejecta component with velocities in excess of $0.6c$ might be responsible for a brighter UV/optical polar emission and a precursor powered by the beta-decay of the free neutrons (Metzger et al. 2015). The dynamical ejecta also generate synchrotron radiation by the shock interaction with the interstellar medium (ISM; e.g., Nakar & Piran 2011; Hotokezaka & Piran 2015; Hotokezaka et al. 2018b); such a radio signature depends on the medium density and on the kinetic energy of the outflow. Current merger simulations cannot self-consistently predict the properties of the secular ejecta, especially because the treatment of key physical processes, such as neutrino-matter interaction and angular momentum transport due to magnetic effects, is limited by the use of approximate schemes and insufficient resolution (e.g., Foucart et al. 2016; Kiuchi et al. 2018). The uncertainties in the theoretical modeling are crucially reflected in the current challenges in the interpretation of the observations.

In this Letter we report the finding of a new outflow mechanism that can operate in unequal mass binaries on dynamical timescales and is enabled by turbulent viscosity. We show that this mechanism can boost the mass of the dynamical ejecta by a factor of a few. The resulting viscous-dynamical ejecta are characterized by their larger-than-typical mass and their distribution extending to high velocities. These outflows could produce UV/optical transients on a timescale of a few hours from the merger, in part powered by the decay of free neutrons in the high-velocity tail of the ejecta. The viscous-dynamical ejecta would also contribute to the overall NIR flux of the KN, and would produce bright radio flares on timescales of weeks to years from the merger. The magnitude of this outflow component for GW170817 could be constrained by future radio observations in the near future.

2. Method

We study the role of the turbulent viscosity in the dynamical ejection of mass during NS mergers using the general-relativistic large eddy simulations method (GRLES; Radice 2017). Viscosity effects are modeled by augmenting the perfect fluid stress-energy tensor with a purely spatial tensor representing the effect of subgrid-scale turbulence. The latter is effectively parametrized by the turbulent viscosity coefficient $\nu_\tau = \ell_{\rm mix} c_s$, where c_s is the sound speed and $\ell_{\rm mix}$ is a free parameter that we vary to study the sensitivity of our results to turbulence. In the context of accretion disk theory turbulent viscosity is typically parametrized in terms of a dimensionless constant, α, linked to $\ell_{\rm mix}$ through the relation $\ell_{\rm mix} = \alpha\, c_s\, \Omega^{-1}$, where Ω is the angular velocity of the fluid (Shakura & Sunyaev 1973).

Recently, Kiuchi et al. (2018) performed very-high-resolution general-relativistic magnetohydrodynamic (GRMHD) simulations of an NS merger with sufficiently high seed magnetic fields (10^{15} G) to resolve the magnetorotational instability (MRI) in the merger remnant and reported averaged α values for different rest mass density shells. Combining their estimate of α with values of c_s and Ω from our simulations, we find values of $\ell_{\rm mix} = 0$–30 m. These values are also consistent with estimates based on dimensional considerations (Duez et al.2006; Radice 2017). Here, we conservatively vary $\ell_{\rm mix}$ between 0 (no subgrid model) and 50 m (very efficient angular momentum transport). On the other hand, we want to emphasize that these estimates for $\ell_{\rm mix}$ have been derived for the post-merger phase and under specific assumptions, such as strong initial magnetic fields and equal masses, while the results presented here depend on the effective viscosity present during the merger for unequal mass systems. Moreover, we caution the reader that in reality $\ell_{\rm mix}$ is likely to be time-dependent and non-constant. For these reasons, our results should only be considered as qualitative until the relevant $\ell_{\rm mix}$ can be estimated, and our approach validated with GRMHD simulations.

We consider two binaries: an equal mass binary with component masses $1.35\,M_\odot$ and $1.35\,M_\odot$, and an unequal mass binary with component masses $1.4\,M_\odot$ and $1.2\,M_\odot$. Notably, this is the first time an unequal mass NS merger simulation has been performed in general relativity (GR) including viscosity. We adopt the LS220 equation of state (EOS; Lattimer & Swesty 1991) that is based on a liquid droplet Skyrme model and predicts a maximum mass of $2.06\,M_\odot$ and radius $R_{1.4}$ of 12.7 km for non-rotating cold NSs. Hence, the EOS is compatible with current astrophysical constraints, including the recent Laser Interferometer Gravitational-Wave Observatory (LIGO)/Virgo constraint on tidal deformability (Abbott et al. 2017a, 2018b, 2018a; De et al. 2018).

We evolve the initial data using the `WhiskyTHC` code (Radice & Rezzolla 2012; Radice et al. 2014a, 2014b, 2015). Neutrinos losses are modeled by a leakage scheme (Galeazzi et al. 2013; Radice et al. 2016), with a free-streaming component evolved according to the M0 scheme introduced in Radice et al. (2016). The M0 scheme models the re-absorption effects and includes approximate gravitational and Doppler effects in a computational efficient way. More technical details are reported in Radice et al. (2018b).

3. Results

The inclusion of viscosity affects the thermodynamical properties of the merger remnants, their lifetimes, and the neutrino luminosities, as discussed in Radice (2017). We focus here only on the dynamical ejecta.

The total ejecta mass for the equal mass $(1.35 + 1.35)M_\odot$ binary does not show a systematic trend with viscosity: we find $0.19 \times 10^{-2}\,M_\odot$, $0.27 \times 10^{-2}\,M_\odot$, $0.20 \times 10^{-2}\,M_\odot$, and $0.20 \times 10^{-2}\,M_\odot$ of dynamical ejecta for the $\ell_{\rm mix} = 0$, 5 m, 25 m, and 50 m simulations, respectively. These differences are at the level expected from the stochastic nature of the mass ejection (Bauswein et al. 2013; Radice et al. 2018b). The intensive properties of the ejecta, i.e., electron fraction, entropy, or on their asymptotic velocities, are also rather insensitive to the inclusion of viscosity. That said, we remark that with the inclusion of turbulent viscosity the mass outflow rate does not drop completely to zero after the merger, as is instead the case for the binaries simulated without the inclusion of viscous angular momentum transport. Instead, the dynamical mass ejection is immediately followed by the early phase of a secular viscous-driven outflow (e.g., Lee et al. 2009; Fernández & Metzger 2013; Metzger & Fernández 2014; Siegel & Metzger 2017; Fernández et al. 2018; Fujibayashi et al. 2018). Our simulations do not extend sufficiently in time to allows us to study the secular ejecta. This will be the subject of our future work.

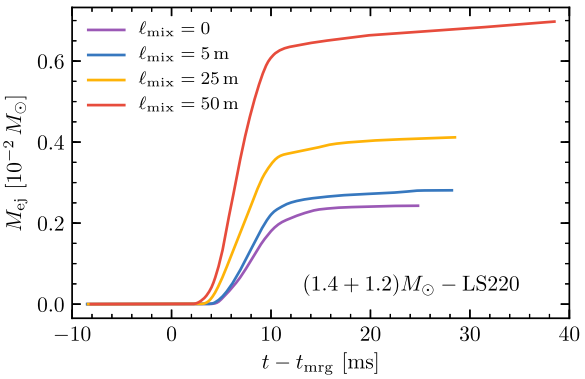

Figure 1. Mass of the dynamical ejecta for the $(1.4 + 1.2)M_\odot$ binary simulated with different values of the viscous parameter $\ell_{\rm mix}$. We find that viscous effects can boost the dynamical ejecta mass by factors of a few.

The case of the unequal mass binary $(1.4 + 1.2)M_\odot$ is qualitatively different and shows a new phenomenon. We find that the dynamical ejecta mass increases monotonically with the viscous parameter $\ell_{\rm mix}$, as shown in Figure 1. The dynamical ejecta mass increases by almost a factor of 3, from $0.24 \times 10^{-2}\,M_\odot$ to $0.7 \times 10^{-2}\,M_\odot$, as the mixing length is increased from 0 to 50 m. The early phase of the secular outflow rate after the merger also grows monotonically with the viscosity. The amount of matter ejected between $t = 15$ ms and $t = 25$ ms, which we tentatively identify with the first part of the secular ejecta, is $0.09 \times 10^{-3}\,M_\odot$, $0.17 \times 10^{-3}\,M_\odot$, $0.20 \times 10^{-3}\,M_\odot$, and $0.24 \times 10^{-3}\,M_\odot$ for the $\ell_{\rm mix} = 0$, $\ell_{\rm mix} = 5$ m, $\ell_{\rm mix} = 25$ m, and $\ell_{\rm mix} = 50$ m runs, respectively. While the increase in the secular ejecta mass with viscosity was expected (e.g., Fujibayashi et al. 2018), the significant growth in the dynamical ejecta mass with viscosity was not.

The origin of the ejecta mass enhancement can be understood from the comparison of the density profiles on the orbital plane for the $\ell = 0$ and $\ell = 50$ m runs shown in Figure 2. We observe the development of mass transfer between the secondary and the primary NSs a few milliseconds prior to the merger. In the simulation with no viscosity, the material outflowing from the secondary settles on the primary NS. The NSs are not corotating, so the accreted material must form a layer on the surface of the primary NS characterized by a large velocity gradient. Viscous heating heats this layer to high temperatures, up to ∼20–30 MeV for $\ell_{\rm mix} = 50$ m. The resulting pressure gradient drives the copious mass outflow. We stress that our fiducial binary has a only moderate mass ratio of $q \simeq 0.85$. Mass transfers are expected to increase for more asymmetric binaries, thus an even larger effect could be expected for smaller q.

The viscous-dynamical ejecta have a broad distribution in Y_e that is very similar to the dynamical ejecta observed in simulations without viscosity (Radice et al. 2018b). This is not too surprising, given that both the shocked and viscous-dynamical ejecta are composed of material from the outer layers of the NSs that is pushed by hydrodynamical forces operating from the interior of the forming merger remnant. In one case the hydrodynamical push is generated by shocks launched after the merger, and in the other by the pressure gradient induced by the viscous heating of the primary NS.

The distinctive features of the viscous-dynamical ejecta are their larger mass and higher asymptotic velocities, the latter up to ∼30% larger than that for the shocked ejecta. Moreover, our simulations show that the amount of fast-moving ejecta with asymptotic velocities larger than $0.6c$ is also significantly increased with the inclusion of viscosity. In the case of the $(1.4 + 1.2)M_\odot$ binary it grows monotonically from $10^{-8}\,M_\odot$ in the run with no viscosity to $8.3 \times 10^{-5}\,M_\odot$ for the run with $\ell_{\rm mix} = 50$ m. A more modest, but still significant, increase in the amount of fast-moving ejecta is also observed for the equal mass binary. In this case the amount of ejecta with asymptotic velocities in excess of $0.6c$ grows from $10^{-7}\,M_\odot$ of the simulation with no viscosity to $0.4 \times 10^{-5}\,M_\odot$ of the simulation with $\ell_{\rm mix} = 50$ m.

4. Discussion

We compute synthetic KN light curves using the semi-analytical model of Perego et al. (2017). Composition, angular distribution, and velocity of the dynamical ejecta are directly taken from the simulations. We also include the contribution of the secular ejecta that we assume to be composed of neutrino-driven wind entraining $0.01\,M_\odot$ of high Y_e material and of $0.05\,M_\odot$ of intermediate Y_e viscous outflows from the remnant's accretion disk. Our model also includes the contribution of free neutron decay following Metzger et al. (2015) and Metzger (2017). In particular, we assume that neutron capture is avoided for ejecta expanding with velocities in excess of $0.6c$ (see Metzger et al. 2015, their Figure 1). We refer to Perego et al. (2017) and Radice et al. (2018b) for a full account of all the inputs to our model.

When considering the $(1.4 + 1.2)M_\odot$ binary, we find that the inclusion of viscosity results in a visible bump in the UV light curve on a timescale of about one hour of the merger. This bump disappears if we switch off the contributions from free neutrons to the emission of the ejecta, so it would be a clear signature of the production of a fast outflow. Overall we find that, because of the presence of free neutrons, the KN could be up to one magnitude brighter in the UV bands in the first hour. This is a somewhat smaller enhancement than that reported by Metzger et al. (2015), who found that free neutrons could boost the brightness of the KN in the UV bands by up to 4 mag. We remark that the peak magnitude in the U-band for our $\ell_{\rm mix} = 50$ m model is consistent with the prediction of Metzger et al. (2015) for the case with $10^{-4}\,M_\odot$ of free neutrons, taking into account differences in assumed opacities, ejecta masses, and expansion velocities. However, possibly because of the more rapid expansion of our ejecta and the presence of low-opacity material at high latitude in our simulations, our synthetic KN light curves are brighter at early times compared with the baseline models of Metzger et al. (2015).

Due to the significant increase of the dynamical ejecta masses, the viscous runs result in modest increases to the KN light curves in the NIR bands by up to ∼0.5 mag (see Figure 3). The reason that the increase in the NIR flux is modest is because the KN is actually dominated by radiation emitted by the secular ejecta on the relevant timescales. This can be seen by comparing the KN light curves computed with the inclusion of both secular and dynamical ejecta with those generated accounting only for the latter. The increase in the amount of high-photon-opacity dynamical ejecta due to viscosity is also inconsequential, because this outflow component is not sufficiently massive and expands too rapidly to significantly obscure the emission from the secular ejecta on a timescale of more than few hours.

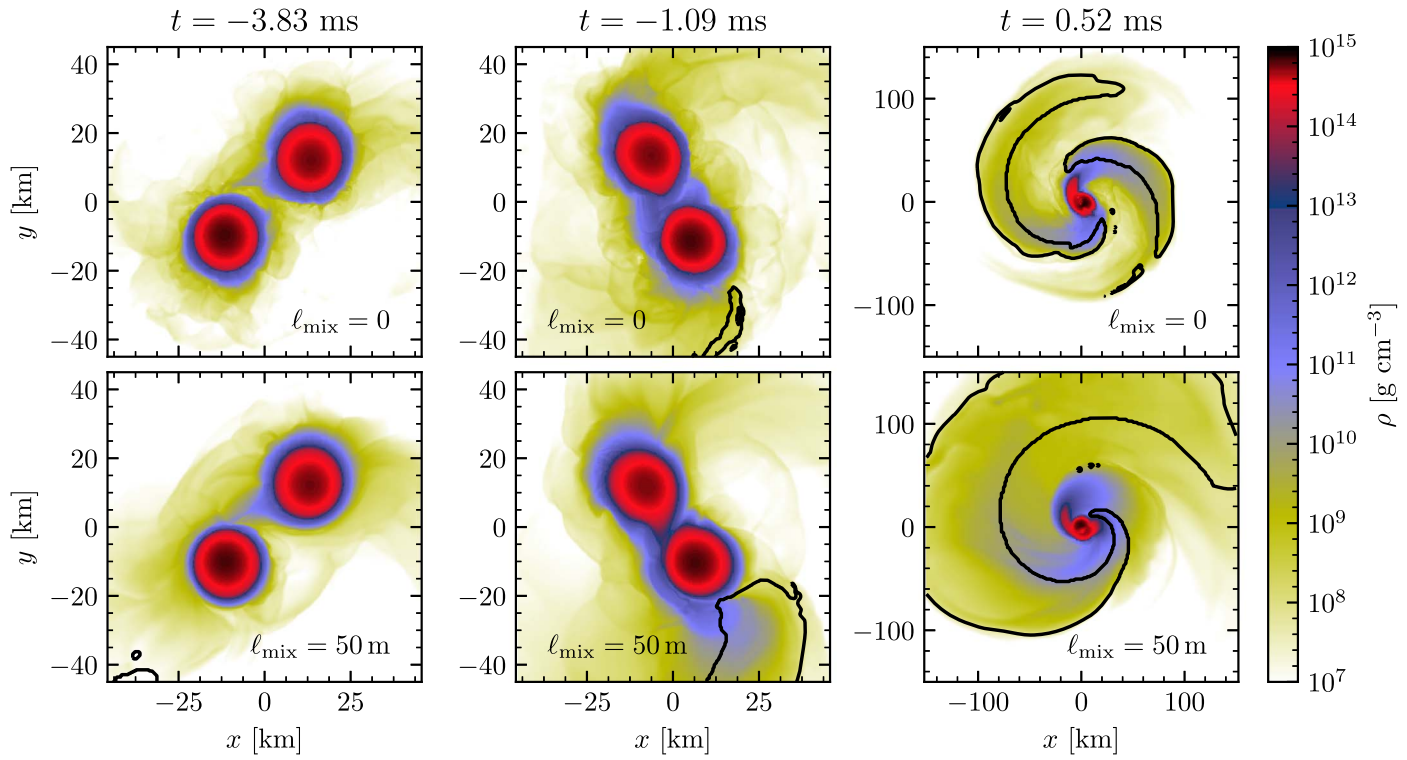

Figure 2. Rest mass density on the orbital plane for the $(1.4 + 1.2)M_\odot$ binary simulated with different values of the viscous parameter $\ell_{\rm mix}$. The black contour denotes unbound material, i.e., with $-u_0 > 1$. Note that more material can become unbound at larger radii. Viscous heating of the tidal stream between the primary and the secondary stars can significantly enhance the mass loss from the binary.

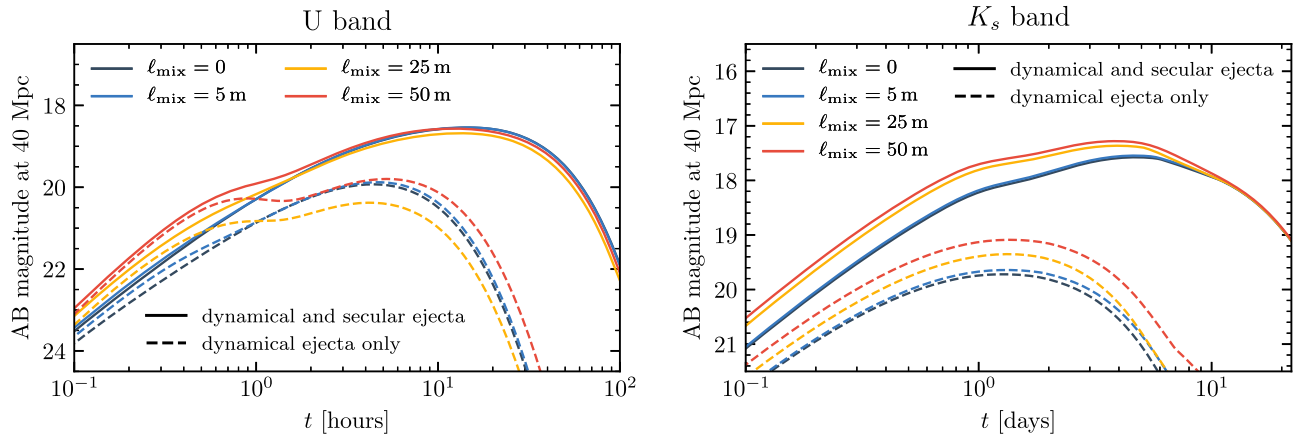

Figure 3. KN light curves for equatorial observers in the U-band (left panel) and K_s band (right panel) for the $(1.4 + 1.2)M_\odot$ binary simulated with different values of the mixing length $\ell_{\rm mix}$. We show light curves obtained accounting only for the dynamical ejecta (dashed lines), and light curves computed including contributions from both the dynamical and the secular ejecta (solid lines). The viscous-dynamical ejecta expands sufficiently rapidly so that free neutron decay can occur and would leave a characteristic bump in the UV/optical light curves in the first hour. The viscous-dynamical ejecta also enhance the flux in the NIR bands at later times.

We estimate the radio light curves from synchrotron emission generated as the ejecta interacts with the ISM using the semi-analytic model of Hotokezaka & Piran (2015). The free parameters of this model are the ISM number density, n, the efficiencies with which the internal energy of the shock is converted into kinetic energy of non-thermal electrons, ϵ_e, and magnetic energy of the amplified background field, ϵ_B. The model assumes spherical symmetry and takes as input the asymptotic velocity distribution of the ejecta.

Our results are shown in Figure 4. The radio light curves are very sensitive to the asymptotic velocity distribution of the ejecta (Hotokezaka et al. 2018b) and, in particular, to the presence of a high-velocity tail. They are also sensitive to the ISM density. In the case of GW170817 the latter is presently constrained to be $\sim 10^{-4}$–$5 \times 10^{-3}\,{\rm cm}^{-3}$ (Ghirlanda et al. 2018; Mooley et al. 2018). We find that the viscous-dynamical ejecta could power radio remnants that are orders of magnitude brighter and peak at earlier times than those predicted by simulations that do not include viscosity. It might be possible to detect or exclude the presence of a large amount of viscous-dynamical ejecta with continued radio observations of GW170817 in the next few years. At the moment, the synchrotron emission from GW170817 is thought to be powered by the interaction between a relativistic jet and the

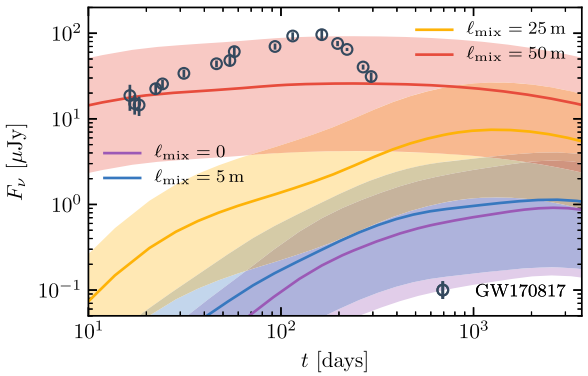

Figure 4. Radio light curves at 3 GHz for the $(1.4 + 1.2)M_\odot$ binary simulated with different values of the mixing length $\ell_{\rm mix}$. The different bands correspond to different models were we vary the ISM density from 10^{-4} cm^{-3} to 5×10^{-3} cm^{-3}, a range compatible with current observational constraints (Mooley et al. 2018). The solid lines correspond to the fiducial value $n = 10^{-3}$ cm^{-3}. Also shown as open circles are the observed flux densities at 3 GHz of the afterglow in GW170817, which is presently dominated by the interaction between a relativistic jet and the ISM (Hallinan et al. 2017; Mooley et al. 2017, 2018). Here we assume the microphysics parameters to be $\epsilon_e = 0.1$, $\epsilon_B = 0.01$, and $p = 2.16$. Viscous-dynamical ejecta could power very bright synchrotron remnants. The $\ell_{\rm mix} = 50$ m simulation predicts a rebrightening of GW170817 in the radio on a timescale of $\sim$1 year from the merger.

ISM (Ghirlanda et al. 2018; Mooley et al. 2018); however, the viscous-dynamical ejecta might be detectable as a break in the decline of the radio data occurring when the emission from the jet will have faded. For mergers occurring in higher-density environments, the radio flares generated by the interaction between the viscous-dynamical ejecta and the ISM could be detected to distances of several tens to few hundreds Mpc.

5. Conclusions

We have shown that the effective viscosity possibly arising from small-scale magnetohydrodynamic turbulence prior to merger can significantly boost the amount of dynamical ejecta for unequal mass binaries. The resulting outflows are neutron rich and have velocity distributions with large mean values and extended tails. These viscous-dynamical ejecta could power KNe showing signatures of free neutron decays on a timescale of about one hour. Indeed, a fraction of the viscous-ejecta, up to $\sim 10^{-4}\,M_\odot$, expands sufficiently rapidly for most neutrons to avoid capture. The resulting heat from the beta-decays would leave a detectable imprint on the KN light curve at early times. The viscous-dynamical ejecta would also contribute to the KN signal in the NIR bands on a timescale of few days. Due to their large kinetic energies, the outflows produced by this new mechanism could also generate very bright radio remnants as they interact with the ISM on longer timescales of weeks to months. Accordingly, it might be possible to constrain the mass and kinetic energy of the viscous-dynamical ejecta for GW170817 with radio observations in the coming months and years.

Whether or not the new ejection mechanism discussed here operates in nature depends on the size of the effective viscosity of the mass exchange flows. At the moment, very rough estimates for the effective viscosity exist only for the post-merger phase of NS mergers, while the mechanism discussed here depends on the effective viscosity of the flow at the time of merger. Understanding this will require very-high-resolution and/or local GRMHD simulations. This will be the subject of future work.

It is a pleasure to acknowledge A. Burrows for the many stimulating discussions, and B. Metzger for comments on an earlier draft of the manuscript. D.R. gratefully acknowledges support from a Frank and Peggy Taplin Membership at the Institute for Advanced Study and the Max-Planck/Princeton Center (MPPC) for Plasma Physics (NSF PHY-1523261). A.P. acknowledges support from the INFN initiative "High Performance data Network" funded by CIPE. D.R. and A.P. acknowledge support from the Institute for Nuclear Theory (17-2b program) and from the Theory Alliance-Facility for Rare Isotope Beams (Topical Program: FRIB and the GW170817 kilonova). A.P. thanks the Institute for Advanced Study for its hospitality and support. S.B. acknowledge support by the EU H2020 under ERC Starting grant No. BinGraSp-714626. S.A.F. acknowledges support from the United States Department of Energy through the Computational Science Graduate Fellowship, grant No. DE-SC0019323. L.F.R. acknowledges support from U.S. Department of Energy through the award number DE-SC0017955. The simulations were performed on BlueWaters, Bridges, Comet, and Stampede, and were enabled by the NSF PRAC program (ACI-1440083 and AWD-1811236) and the NSF XSEDE program (TG-PHY160025). The analysis employed computational resources provided by both the TIGRESS high performance computer center at Princeton University, which is jointly supported by the Princeton Institute for Computational Science and Engineering (PICSciE) and the Princeton University Office of Information Technology, and the Institute for Cyber-Enabled Research, which is supported by Michigan State University.

ORCID iDs

David Radice https://orcid.org/0000-0001-6982-1008
Albino Perego https://orcid.org/0000-0002-0936-8237
Kenta Hotokezaka https://orcid.org/0000-0002-2502-3730
Sebastiano Bernuzzi https://orcid.org/0000-0002-2334-0935

References

Abbott, B. P., Abbott, R., Abbott, T. D., et al. 2017a, PhRvL, 119, 161101
Abbott, B. P., Abbott, R., Abbott, T. D., et al. 2017b, ApJL, 848, L12
Abbott, B. P., Abbott, R., Abbott, T. D., et al. 2018a, PhRvL, 121, 161101
Abbott, B. P., Abbott, R., Abbott, T. D., et al. 2018b, arXiv:1805.11579
Bauswein, A., Goriely, S., & Janka, H. T. 2013, ApJ, 773, 78
Chornock, R., Berger, E., Kasen, D., et al. 2017, ApJL, 848, L19
Cowperthwaite, P. S., Berger, E., Villar, V. A., et al. 2017, ApJL, 848, L17
Davies, M. B., Benz, W., Piran, T., & Thielemann, F. K. 1994, ApJ, 431, 742
De, S., Finstad, D., Lattimer, J. M., et al. 2018, PhRvL, 121, 091102
Dessart, L., Ott, C., Burrows, A., Rosswog, S., & Livne, E. 2009, ApJ, 690, 1681
Drout, M. R., Piro, A. L., Shappee, B. J., et al. 2017, Sci, 358, 6370
Duez, M. D., Liu, Y. T., Shapiro, S. L., & Shibata, M. 2006, PhRvD, 73, 104015
Eichler, D., Livio, M., Piran, T., & Schramm, D. N. 1989, Natur, 340, 126
Fernández, R., & Metzger, B. D. 2013, MNRAS, 435, 502
Fernández, R., Tchekhovskoy, A., Quataert, E., Foucart, F., & Kasen, D. 2018, arXiv:1808.00461
Foucart, F., O'Connor, E., Roberts, L., et al. 2016, PhRvD, 94, 123016
Freiburghaus, C., Rosswog, S., & Thielemann, F.-K. 1999, ApJL, 525, L121
Fujibayashi, S., Kiuchi, K., Nishimura, N., Sekiguchi, Y., & Shibata, M. 2018, ApJ, 860, 64
Fujibayashi, S., Sekiguchi, Y., Kiuchi, K., & Shibata, M. 2017, ApJ, 846, 114
Galeazzi, F., Kastaun, W., Rezzolla, L., & Font, J. A. 2013, PhRvD, 88, 064009

Ghirlanda, G., Salafia, O. S., Paragi, Z., et al. 2018, arXiv:1808.00469
Goriely, S., Bauswein, A., & Janka, H. T. 2011, ApJL, 738, L32
Hallinan, G., Corsi, A., Mooley, K. P., et al. 2017, Sci, 358, 6370
Hotokezaka, K., Beniamini, P., & Piran, T. 2018a, IJMPD, 27, 1842005
Hotokezaka, K., Kiuchi, K., Kyutoku, K., et al. 2013, PhRvD, 87, 024001
Hotokezaka, K., Kiuchi, K., Shibata, M., Nakar, E., & Piran, T. 2018b, ApJ, 867, 95
Hotokezaka, K., & Piran, T. 2015, MNRAS, 450, 1430
Just, O., Bauswein, A., Pulpillo, R. A., Goriely, S., & Janka, H. T. 2015, MNRAS, 448, 541
Kasen, D., Metzger, B., Barnes, J., Quataert, E., & Ramirez-Ruiz, E. 2017, Natur, 551, 7678
Kawaguchi, K., Shibata, M., & Tanaka, M. 2018, ApJL, 865, L21
Kiuchi, K., Kyutoku, K., Sekiguchi, Y., & Shibata, M. 2018, PhRvD, 97, 124039
Korobkin, O., Rosswog, S., Arcones, A., & Winteler, C. 2012, MNRAS, 426, 1940
Lattimer, J. M., & Schramm, D. N. 1974, ApJL, 192, L145
Lattimer, J. M., & Swesty, F. D. 1991, NuPhA, 535, 331
Lee, W. H., Ramirez-Ruiz, E., & López-Cámara, D. 2009, ApJL, 699, L93
Lippuner, J., Fernández, R., Roberts, L. F., et al. 2017, MNRAS, 472, 904
Martin, D., Perego, A., Arcones, A., et al. 2015, ApJ, 813, 2
Metzger, B. D. 2017, LRR, 20, 3
Metzger, B. D., Bauswein, A., Goriely, S., & Kasen, D. 2015, MNRAS, 446, 1115
Metzger, B. D., & Fernández, R. 2014, MNRAS, 441, 3444
Metzger, B. D., Piro, A. L., & Quataert, E. 2008, MNRAS, 390, 781
Metzger, B. D., Piro, A. L., & Quataert, E. 2009, MNRAS, 396, 304
Metzger, B. D., Thompson, T. A., & Quataert, E. 2018, ApJ, 856, 101
Meyer, B. S. 1989, ApJ, 343, 254
Mooley, K. P., Deller, A. T., Gottlieb, O., et al. 2018, Natur, 561, 7723
Mooley, K. P., Nakar, E., Hotokezaka, K., et al. 2017, Natur, 554, 7691
Nakar, E., & Piran, T. 2011, Natur, 478, 82
Nicholl, M., et al. 2017, ApJL, 848, L18
Perego, A., Radice, D., & Bernuzzi, S. 2017a, ApJL, 850, L37
Perego, A., Rosswog, S., Cabezón, R. M., et al. 2014, MNRAS, 443, 3134
Perego, A., Yasin, H., & Arcones, A. 2017b, JPhG, 44, 084007
Radice, D. 2017, ApJL, 838, L2
Radice, D., Galeazzi, F., Lippuner, J., et al. 2016, MNRAS, 460, 3255
Radice, D., Perego, A., Bernuzzi, S., & Zhang, B. 2018a, arXiv:1803.10865
Radice, D., Perego, A., Hotokezaka, K., et al. 2018b, arXiv:1809.11161
Radice, D., & Rezzolla, L. 2012, A&A, 547, A26
Radice, D., Rezzolla, L., & Galeazzi, F. 2014a, MNRAS, 437, L46
Radice, D., Rezzolla, L., & Galeazzi, F. 2014b, CQGra, 31, 075012
Radice, D., Rezzolla, L., & Galeazzi, F. 2015, in ASP Conf. Ser. 498, Numerical Modeling of Space Plasma Flows ASTRONUM-2014, ed. N. V. Pogorelov et al. (San Francisco, CA: ASP), 121
Rosswog, S., & Davies, M. B. 2003, MNRAS, 345, 1077
Rosswog, S., Liebendoerfer, M., Thielemann, F. K., et al. 1999, A&A, 341, 499
Rosswog, S., Piran, T., & Nakar, E. 2013, MNRAS, 430, 2585
Rosswog, S., Sollerman, J., Feindt, U., et al. 2018, A&A, 615, A132
Sekiguchi, Y., Kiuchi, K., Kyutoku, K., & Shibata, M. 2015, PhRvD, 91, 064059
Sekiguchi, Y., Kiuchi, K., Kyutoku, K., Shibata, M., & Taniguchi, K. 2016, PhRvD, 93, 124046
Shakura, N. I., & Sunyaev, R. A. 1973, A&A, 24, 337
Siegel, D. M., Ciolfi, R., & Rezzolla, L. 2014, ApJL, 785, L6
Siegel, D. M., & Metzger, B. D. 2017, PhRvL, 119, 231102
Siegel, D. M., & Metzger, B. D. 2018, ApJ, 858, 52
Symbalisty, E., & Schramm, D. N. 1982, ApJL, 22, L143
Tanaka, M., Utsumi, Y., Mazzali, P. A., et al. 2017, PASJ, 69, 102
Tanvir, N. R., Levan, A. J., González-Fernández, C., et al. 2017, ApJL, 848, L27
Thielemann, F. K., Eichler, M., Panov, I. V., & Wehmeyer, B. 2017, ARNPS, 67, 253
Villar, V. A., Guillochon, J., Berger, E., et al. 2017, ApJL, 851, L21
Wanajo, S., Sekiguchi, Y., Nishimura, N., et al. 2014, ApJL, 789, L39
Waxman, E., Ofek, E., Kushnir, D., & Gal-Yam, A. 2017, arXiv:1711.09638
Wu, M.-R., Fernández, R., Martínez-Pinedo, G., & Metzger, B. D. 2016, MNRAS, 463, 2323